Low frequency magnetic variations at high-β Earth bow shocks

Anatoli A. Petrukovich[1], Olga M. Chugunova[1], and Pavel I. Shustov[1]

[1]Space Research Institute of Russian Academy of Sciences, Moscow, Russia

Correspondence: A.A.Petrukovich (a.petrukovich@cosmos.ru)

Abstract. Earth's bow shock ~~in~~ high β (ratio of thermal to magnetic pressure) solar wind ~~environment is a~~ rare ~~phenomenon~~. However such an object is ubiquitous in astrophysical plasmas. Typical solar wind parameters related with high β (here $\beta > 10$) are: low speed, high density and very low IMF 1–2 nT. These conditions are usually quite transient and need to be verified immediately upstream of the observed shock crossings. About a hundred high-β shocks were initially identified during 1995–2016 mostly with oblique or quasi-perpendicular geometry and high Mach number. In this report 22 crossings by Cluster project are studied with multipoint analysis, allowing to determine spatial scales. **The main magnetic field and density increase is smeared ~~to the length~~ of couple tens of seconds (couple of hundred km). Dominating magnetic variations in the shock transition have amplitudes much larger than the background field and frequency of ~0.3–0.5 Hz (in some events — 1–2 Hz). This ~~layout~~ is quite characteristic for the studied shock type. Their polarization has no stable phase and is closer to linear, complicating determination of the wave propagation direction. Spatial scales of variations are within several tens to couple hundred km.**

1 Introduction

Shocks are the primary dissipation mechanism in space plasmas with supersonic flows (Sagdeev, 1966; Kennel et al., 1985; Krasnoselskikh et al., 2013). A ~~brand~~ new branch of plasma science, theory of collisionless shocks, appeared in the sixties, in response to new space observations. Solar wind forms bow shocks at planets and comets, as well as the termination shock at the heliospheric interface. Interplanetary shocks develop inside the heliosphere after solar eruptions, when large-scale transient structures propagate relative to the regular solar wind flow. In ~~the~~ distant space, shocks are associated with supernova explosions, stellar winds, collisions of galaxy clusters and are believed to have a leading role in the acceleration process of cosmic rays (Axford et al., 1977; Krymskii, 1977). Physics of space shocks was reviewed in AGU Geophysical Monographs, volumes 34 and 35 (1985). The Earth bow shock has been most thoroughly studied and is the main source of our in-situ knowledge of collisionless shock structure and dynamics.

Electromagnetic fields and waves in collisionless plasma shocks are of primary importance. Due to presence of magnetic field wide variety of shock types exists with quite differing structure (Kennel et al., 1985). Magnetic field vector ~~enters~~

Rankine-Hugoniout equations, defining the relation between upstream and downstream conditions. In the absence of collisions, kinetic mechanisms of field-particle interactions are responsible for dissipation and particle acceleration (Sagdeev, 1966; Krasnoselskikh et al., 2013). With quasi-perpendicular shock geometry (when the angle between the shock normal and the upstream magnetic field is closer to 90^o) ions cannot escape upstream and relatively sharp shock transition forms with the ion-scale overall width (several thousand km). ~~With~~ quasi-parallel geometry (the angle is closer to 0^o) ions easily escape upstream along magnetic field and shock transition smears to the scales around several Earth radii (Scudder et al., 1986; Burgess et al., 2005). Oblique shocks (angles around 45^o) are in a sense intermediate in properties, when ions partially are capable to escape upstream, but generally have rather spatially localized transition similar to quasi-perpendicular ones.

Besides this large-scale magnetic field structure, also of interest at the Earth's bow shock are relatively low frequency magnetic variations (from one tenth to few Hz) with visually maximal amplitudes, which actually form the primary shock front structure, dissipating ions. For example, in a supercritical quasi-perpendicular shock, the oblique whistler waves near the lower-hybrid frequency (~5 Hz) form the magnetic ramp via the non-linear steepening and decay cycle (Krasnoselskikh et al., 2002, and references therein). In the several studies the wavelength of these waves and the scale of shock ramp were determined to be around 10-s of km and oscillations were in fact identified as whistlers (Petrukovich et al., 1998; Walker et al., 2004; Hobara et al., 2010; Schwartz et al., 2011; Dimmock et al., 2013; Krasnoselskikh et al., 2013). Cyclic shock reformation is typical also for quasi-parallel shocks with substructures known as SLAMS and oblique shocks (Lefebvre et al., 2009). Specifics of a plasma wave mode driving the front reformation depends of local plasma parameters, Mach number, etc. Immediately downstream of the shock front plasma waves at the frequencies below the ion cyclotron one were attributed to mirror, ion cyclotron, intermediate modes (e.g., Balikhin et al., 1997; Czaykowska et al., 2001). Yet one more issue of interest is electron heating. It requires sufficiently small scale variations for non-adiabatic acceleration and ~~following~~ isotropisation (Balikhin et al., 1993; Vasko et al., 2018).

Of interest to some astrophysical applications are shocks in a weak magnetic field environment (high-β shocks), common in interstellar and intergalaxy space (e.g., Markevitch and Vikhlinin, 2007; Donnert et al., 2018). β is a dimensionless parameter, a ratio of plasma thermal to magnetic energy density. For low background magnetic fields, shock-associated variations may be also considered as kind of 'magnetic field amplification', increasingly important for particle heating. Unfortunately, observations of high β shocks near Earth are quite rare, since the solar wind plasma usually has $\beta \sim 1$.

In our study we take $\beta > 10$ as threshold of high β, this choice is explained further below. Very few investigations of high-β shocks ~~were~~ published. Coroniti (1970) in a theoretical study suggested Alfvén mode to dominate downstream such a shock. Formisano et al. (1975) presented three cases of OGO-5 spacecraft observations with β equal to 8, 170, 49. General ~~layout~~ of these crossings was discussed and large magnetic field excursions up to 20 times larger than IMF were reported. Presence of some transient 'precursor activations' upstream of the main transitions was interpreted as a sign of principal nonstationarity of a shock structure. It was concluded that despite formal high β, magnetic field should not be ignored in theory studies of shock structure. Winterhalter and Kivelson (1988) stated that high-amplitude magnetic variations, which are larger than the main magnetic jump, are typical for the cases with higher β. However specific examples of interest to our study were not shown. Farris et al. (1992) investigated one shock with β equal to 18,

checking validity of Rankine-Hugoniot conditions and also mentioning high-amplitude magnetic variations. However, neither of these studies studied in detail these variations at shock transition zone. Finally, we also note, that in some, rather numerous, investigations moderate $\beta \geq 1$ was termed as "high-β" regime (e.g., $\beta = 2.4$ in Scudder et al., 1986).

We perform an extended experimental study of high-β bow shocks, with a first, to the best of our knowledge, multi-point analysis of dominating low-frequency magnetic varations at high-β shock transition using observations of Cluster project. To access possible solar wind variability we use also ACE and Wind final Earth-shifted data from OMNI-2 archive. Though such solar wind statistics is generally known (review in Wilson et al., 2018), some issues relevant to shock identification and analysis are still worth addressing. All vectors are in GSE frame of reference.

2 Solar wind statistics and details of search procedure

We use 1-hour OMNI-2 data for the period 1995–2017 to determine occurrence of high β solar wind for the subsequent shock analysis. **β values are precalculated in OMNI-2, assuming constant electron temperature (140000 K), He++ fraction (0.05) and He++ temperature (four times larger than proton temperature).** The average solar wind β is somewhat larger than unity. High β conditions are unevenly distributed across solar cycles (Fig. 1), being more frequent at the solar minima 1996–1997 and 2007–2009. For the threshold $\beta > 10$ there are 50–500 hours per year, while for $\beta > 20$, the number is about 3–5 times smaller.

Figure 2 shows distributions of magnetic field magnitude, solar wind speed, density and total static pressure for the full dataset of one-hour values during 1995–2017 and for the subset $\beta > 10$. High β corresponds to slow, cold and dense solar wind with low magnetic field (ion temperature not shown here). However the total static (magnetic plus thermal) pressure distribution is similar (Fig. 2b). Thus the high-β events are mostly depressions of magnetic field, compensated (at least on average) by increase of plasma density. The only notable difference of distributions for $\beta > 20$ (Fig. 2a, red line) is more frequent presence of magnetic field $\sim$1 nT, with the average 1.6 nT, while for $\beta > 10$ the average is $\sim$2.2 nT.

More than 50% of events with $\beta > 10$ have one-hour duration (one point in the analysed OMNI variant, not shown here). A sample event is in Fig. 3 (here 1-min OMNI-2 variant is used). There is about one-hour long decrease of magnetic field and density increase, corresponding to $\beta \sim 20$. At an occasional depletion of magnetic field below 2 nT β jumps to about 40–80 for few minutes. Since formation of high β conditions mostly depends on subtle variations of magnetic field magnitude around 1–2 nT (note, that β has square dependence on magnetic field), it should be quite sensitive to spatial inhomogeneity of solar wind and IMF, and, in particular, to differences between those detected at L1 (in OMNI dataset) and actually hitting Earth. **Fig. 4 shows comparison of β calculation for Wind and ACE 1-hour data (only for times, when Wind data were used in OMNI). The scatter is indeed large. For this OMNI-2 subset there were 618 1-hour points with $\beta > 10$ either in Wind or ACE data. Only for 196 of them difference between β at two spacecraft was less than 30%. For more than half of events (318) difference between the spacecraft was larger than 50%.**

We formulate several conclusions important for our specific shock analysis. (1). Solar wind intervals with high $\beta = 10$–20 are rare, but not extremely rare, and occur mostly during solar minimum. Thus some spacecraft (or the project phases with the

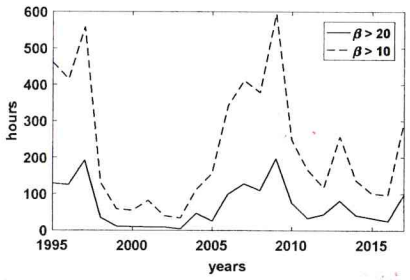

Figure 1. Number of hours with high β with respect to calendar year.

specific orbit or spacecraft separation) may almost completely miss such events. (2). Duration of intervals of interest is relatively short, thus selection of shocks with stable upstream conditions may be not always possible. (3). Very low interplanetary magnetic field, necessary for high-β events, is subject to strong (in relative terms) intrinsic spatial and temporal variability, thus actual β conditions and IMF vector need to be always rechecked with local measurements. This issue is further illustrated with the event selection results below and is elaborated more in Discussion.

Since the high-β shocks are rare, it is unreasonable to search for them, rechecking every registered event. It is more practical first to identify the intervals with the suitable conditions of solar wind. The semi-automated algorithm is used to assemble initial statistics of the shock candidates. For each 1-hour point in OMNI with $\beta > 10$, we check for possible spacecraft location within 5 R_E from the model bow shock (Farris et al., 1991). We scanned 1995–2017 observations by all available spacecraft. For this initial selection we use orbital data and spin-averaged magnetic field data from CDAWeb archive.

In a case any spacecraft is in the right place, the plots of solar wind, IMF, local magnetic field and plasma parameters are analyzed visually in the 5-hour window around the selected hour. These broad temporal and spatial spans are used to ensure that all possible crossings of a moving bow shock are captured for future analysis. Only events with the clear shock traversals (jumps in magnetic field and ion density) are accepted. Such a manual selection has definite bias to quasi-perpendicular and oblique shocks (which usually have a step-like appearance), but it is considered acceptable for this particular study. The most of these initially selected intervals actually contain no shock crossings.

Discovered particular shock crossings are checked with 1-min OMNI data. Plasma β is often below 10, either because registered shocks are just outside of initially selected hours, or because β varied on a time scale smaller than an hour. Since a change of β is usually accompanied with the solar wind density change, there is a dynamic pressure change also. The latter drives large-scale shock motion and probability of shock registration by a spacecraft increases. In fact, many shock crossings are registered at a boundary of β change and such events are also discarded, since it is impossible to attribute them to stable upstream plasma conditions.

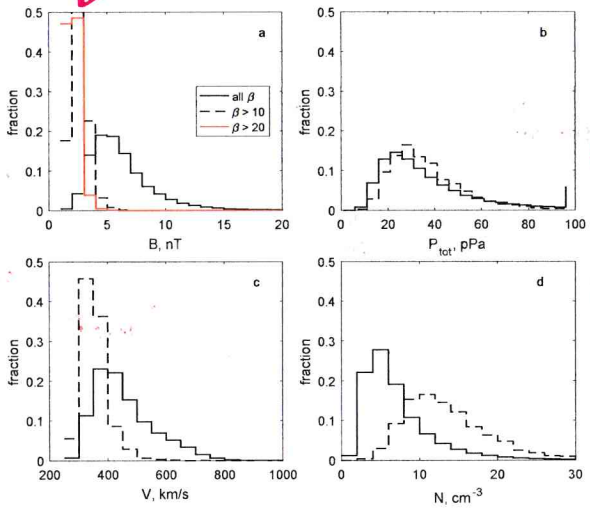

Figure 2. Histograms of solar wind and IMF occurrence for 1995–2017 (solid lines) and for $\beta > 10$ (dashed lines) subset. (a) Total magnetic field (red line corresponds to $\beta > 20$) , (b) total static pressure, (c) solar wind speed, (d) ion density.

Finally the list contained about a hundred individual crossings with average β about 20 (taken as 1-min OMNI value at the moment of shock front crossing). About ten events occurred with very high $\beta > 40$. The choice of initial threshold $\beta > 10$ (for 1-hour points) was finally justified at this stage, since a variant with initial $\beta > 20$ resulted with the almost empty list. However, all these events still need a more detailed confirmation, in particular, of local high β, stable enough crossing velocity, plasma data availability etc.

For the specific multipoint analysis in this investigation we selected 22 verified Cluster project crossings with relatively small spacecraft separation. The full list is in Table S1 in Supplement 1. **For the detailed analysis we used full-resolution Cluster FGM magnetic field (here with the sampling ~20 Hz) (Balogh et al., 2001) and HIA/CODIF ion data (sampling once in 8 seconds) (Rème et al., 2001) from Cluster Science Archive.** One event is from 2003, with the Cluster tetrahedron size of about 300 km, while the other are for the late years 2008–2016, when separation only between a pair of Cluster spacecraft C3 and C4 was controlled (30–150 km for our events). This uneven annual distribution is a consequence of the solar cycle dependence (Fig. 1). Events are grouped in 7 days. Specifically, 5 crossings are registered within one hour at December 18, 2011, 4 crossings — within two hours at January 3, 2008, 8 crossings — within two hours at January 4, 2008, 2 crossings

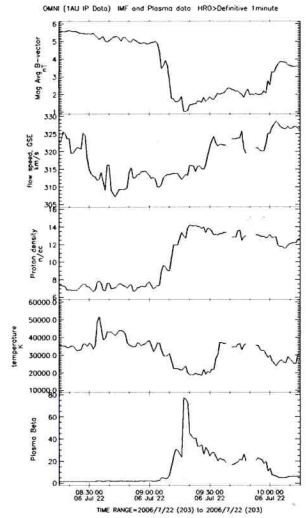

Figure 3. Example of high-β interval. From top to down: magnetic field magnitude, solar wind speed, proton density, proton temperature, plasma β. 1-min OMNI data set used.

— within one hour at February 16, 2012. However not all these adjacent crossings are similar. Some of these examples are presented below.

3 Shock examples

3.1 Event 1

The first example is registered by Cluster C3 and C4 spacecraft on 18 December 2011 (14:36–14:40 UT) with the separation 36 km. The spacecraft orbit is almost parallel to the model shock front (Fig. 5), but shock velocity is definitely much higher than the spacecraft velocity. Fig. 6 contains overview of magnetic field and plasma parameters. Solar wind speed is small ~260 km/s, IMF magnitude — 2.5 nT (all characteristics are in Table S1). Alfvén Mach number is ≈18, magnetosonic Mach number is ≈5, β (according to 1-min OMNI) is 10.8.

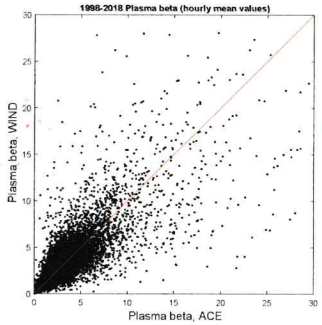

Figure 4. Comparison of Wind and ACE β using 1-hour data. See text for details. Red line is bisector

Cluster ion (proton) density in solar wind is lower than that in OMNI, however WHISPER electron density is almost the same. Proton perpendicular temperature grows as expected towards downstream, while the parallel temperature peaks just upstream the shock front. We attribute this peak to the upstream-moving field-aligned ions. Presence of two populations with strongly different flow velocity results in the false temperature increase. Thus using local ion data to calculate local β would be unreliable. We confirm β using local magnetic field only, since it is the most variable parameter (in comparison with the plasma density). Solar wind magnetic field measured locally by Cluster is the same as OMNI data (compare two lines in Fig. 6d), therefore OMNI β value is confirmed. OMNI IMF vector direction is only $\sim 10^o$ different with the local upstream field taken at 14:40–14:41 UT (not shown here). The model shock normal angle with respect to OMNI (local) IMF θ_{Bn} is 46^o (54^o) (using Farris et al. (1991) model). The coplanarity calculation for the shock normal results in $\theta_{Bn} = 42^o$. Thus this is quasi-perpendicular or oblique supercritical bow shock with the reliably determined geometry. Its structure for more standard β is well studied (Scudder et al., 1986; Krasnoselskikh et al., 2013; Lefebvre et al., 2009). The final value of downstream magnetic field is around 10 nT, and compression ratio is thus close to maximally possible value of 4, in accordance with the high Mach number.

The shock transition lasts about 200 seconds (14:37:00–14:40:30 UT) from the first signs of gyrating ions upstream (Fig. 6f) up to the stable downstream conditions. The increase in magnetic field magnitude (aka shock ramp in a quasi-perpendicular case) is smeared within half a minute (14:37:45-14:38:20 UT) and is accompanied with the similar smeared increase of ion density. The nominal shock front transition is somewhat arbitrarily placed at 14:37:45 UT (marked by vertical line) at a first extended peak of magnetic field. The magnetic field increase is wavy, rather than regular or step-like, magnetic magnitude immediately downstream is often down to 5 nT. Thus it is impossible to determine the shock speed, comparing C3 and C4 measurements.

However, Cluster 2, being about 6000 km away from the pair C3 and C4, crossed the shock two minutes later (exact values are 6231 km and 124 s between C3 and C2, not shown here). The separation along the model normal is 1032 km, the spacecraft are placed almost along the shock front. Shock velocity along the normal is 8.3 km/s outbound. This calculation is not very reliable for two reasons: (1) The spacecraft are mostly separated along the front by about 6000 km, shock motion may be different in two so different points. (2) The reverse crossings occurred less than 10 min later, thus the shock speed might substantially change on a scale of two min (separation between C3 and C2). Nevertheless, one can estimate the spatial scale of the smeared ramp. Duration of 35 s corresponds to 290 km. The gyroradius of solar wind proton is ~700 km, ion inertial length in solar wind is ~80 km.

Despite the described smeared magnetic field increase, the full shock transition is rather compact and coherent and thus it is distinctly different from what expected for quasi-parallel shock with multiple shocklets (Burgess et al., 2005).

We highlight in Figure 7 the interval with the strongest low-frequency magnetic variations. Frequency spectra are in Figure 8. The magnetic profile is dominated by a variation with frequency around 0.3 Hz and amplitude up to 20 nT, more pronounced in B_y. An interval 14:37:27–14:37:47 is taken to estimate the wavelength. The main oscillation (0.3 Hz) is very similar at two spacecraft and visually the time shift between C3 and C4 is about a fraction of a second. Since the variation has a clear dominating frequency, it is more convenient to perform the time-domain multi-point analysis.

Parameters of magnetic variations, filtered in frequency range 0.1–0.77 Hz, are in Table 1. The vector of maximum variance is almost along local magnetic field (B_y component dominates), of minimum variance — along Z. Ratios of eigenvalues are $\lambda_{min}/\lambda_{int} = 0.34$, $\lambda_{int}/\lambda_{max} = 0.58$, and one may assume elliptic polarization. The time shift between magnetic measurements along the maximum variance component, determined with the correlation analysis, is 0.13 s. This value is rather reliably calculated, since it is 2–3 times larger than the sampling interval. The spacecraft separation along the minimum variance direction is 10 km and the resulting wavelength estimate is ~250 km. However the hodograph of magnetic field rotation (Fig. 9) shows that the polarization actually might be linear with the variable eigenvector (but mostly along the determined maximum variance). In such a case the propagation direction cannot be defined with the variance analysis. For the compressive low frequency MHD waves the propagation direction can be determined with the coplanarity approach (Hubert et al., 1998). The maximum variance direction, the magnetic field direction and the wavevector should be in the same plane. However, in our case, the angle between the maximum variance direction and the local magnetic field is rather small (only 12^o) and coplanarity calculation result would be unrealiable.

We also estimate the span of principally possible wavelengths. The maximal one is ~900 km, obtained taking full spacecraft separation 36 km. The Doppler shift is 0.04–0.58 Hz, depending on wavelength and taken local proton velocity value (full 146 km/s or its projection to minimal eigenvector 41 km/s).

Finally we note the oscillations with higher frequency about 1 Hz and smaller amplitude of couple nT, which are best observable in B_z component (Fig. 7c and Fig. 8). The eigenvalue ratios (after filtering the frequency range 0.7–10 Hz) are $\lambda_{min}/\lambda_{int} = 0.68$, $\lambda_{int}/\lambda_{max} = 0.49$, thus reliable determination of any wave proper direction is definitely not possible. Oscillations are quite different at two spacecraft and the multipoint analysis also proved to be not possible.

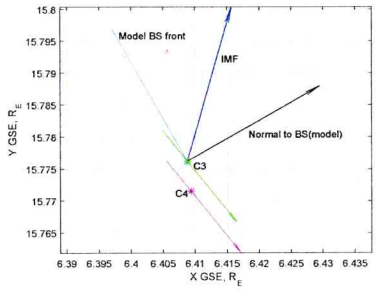

Figure 5. Spacecraft orbit and model shock position for shock 12 December 2011.

Table 1. Wave analysis data for shock 18 December 2011, 14:37:27–14:37:47.

max eigenvector, V_{max}	-0.23, 0.94, 0.27
med eigenvector, V_{med}	0.97, 0.20, 0.15
min eigenvector, V_{min}	-0.08, -0.29, 0.95
eigenvalues	2.23, 6.64, 11.50
magnetic field C3, B_3 (nT)	-3.58, 9.53, 0.96
local proton velocity C4 (km/s)	-118.1, 82.1, -29.29
angle, V_{max} and IMF	34^o
angle, V_{min} and IMF	110^o
angle, V_{max} and B_3	12^o
angle, V_{min} and B_3	99^o
peak frequency in max component	0.3 Hz
time shift in magnetic field along V_{max}	0.13 s
separation along V_{min}	10 km
wavelength	252 km

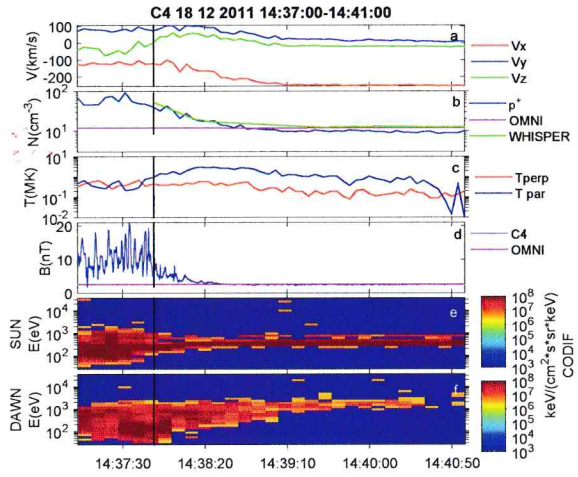

Figure 6. Overview of C4 magnetic and plasma (CODIF) measurements for event 18 December 2011. (a) proton velocity, (b) proton density, OMNI solar wind density, WHISPER electron density, (c) proton parallel and perpendicular temperature, (d) magnetic field magnitude and OMNI IMF magnitude, (e,f) proton spectrograms for the sunward and dawnward looking sectors.

3.2 Event 2

A shock from January 4th, 2008 (16:00–16:04 UT) was registered with Cluster C3 and C4 separation about 40 km. General event parameters are in Table S1, the overview of plasma and magnetic field parameters is in Fig.S1 in Supplement. The detailed wave activity at the front is presented in Fig. 10. Solar wind parameters and general crossing structure are very similar to that for Event 1. Solar wind speed is small ~315 km/s, IMF magnitude — 2.4 nT. Alfvén Mach number is ≈23, magnetosonic Mach number is ≈7, β (according to 1-min OMNI) is 12.2. Solar wind magnetic field measured locally by Cluster is the same as OMNI data (compare two lines in Fig. S1d), therefore OMNI β value is confirmed. All variants for θ_{Bn} give ~40°.

The transition lasts about 2 minutes 16:00:50-16:02:50 from the first signs of gyrating ions upstream to the stable downstream conditions (Fig. S1f). The jump in magnetic field magnitude and ion density is smeared within half a minute 16:01:30-16:02:00 UT, and is wavy rather than step-like, downstream magnetic magnitude is often as small as 2–5 nT. The nominal shock front transition is somewhat arbitrarily placed at 16:01:35 UT at a first extended peak of magnetic field.

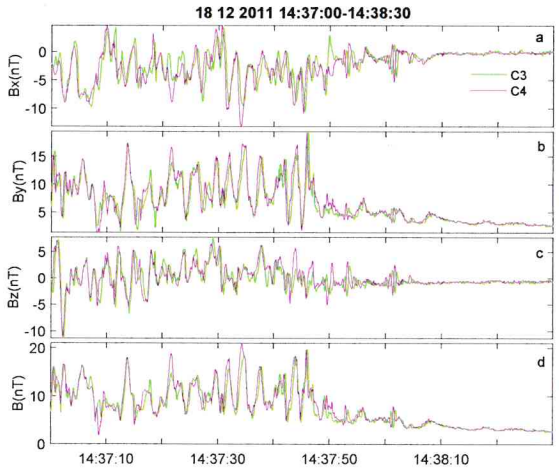

Figure 7. Full resolution magnetic waveform for shock 18 December 2011. In panels (a-d) are components and total value of magnetic field.

Similar to Example 1, one can estimate shock speed along the normal, comparing with C2 crossings (not shown here). However for this example, the spacecraft separation is more than 11000 km, while the separation along the model normal is much smaller, just about 100 km. The estimated shock speed is 1.5–2.2 km/s (comparing the pairs C3-C2 and C4-C2), corresponding to the smeared ramp width about 50 km. However this estimate is very unreliable, since this calculation result would strongly depend on small variations of the actual normal.

The full resolution waveform is in Figure 10. Similar to Event 1, there is a dominating oscillation with the frequency about 0.4–0.5 Hz, as well as the lower amplitude waves with the frequency above 1 Hz (Fig. S2). **The specific feature of this event is an ultimate difference of C3 and C4 variations during the first 20 s downstream the front (16:01:25–16:01:35 UT), despite relatively small separation. The substantial difference in waveforms remains also further downstream. This specifics of variations typical for all shocks registered during this day (8 crossings within 2 hours in Table S1).**

Despite these differences, it is possible to perform multipoint separation analysis for the interval 16:01:15-16:01:25 UT, where two waveforms in B_y component (Fig. 10b) are ~~kind of~~ similar and shifted by a fraction of period. All wave parameters (filtered in the range 0.1–2 Hz) are in Table 2. As in Event 1, maximum eigenvector is almost along Y, medium eigenvector — along X. Ratios of eigenvalues are $\lambda_{min}/\lambda_{int} = 0.15$, $\lambda_{int}/\lambda_{max} \approx 0.5$, thus the minimum variance (nominal propagation)

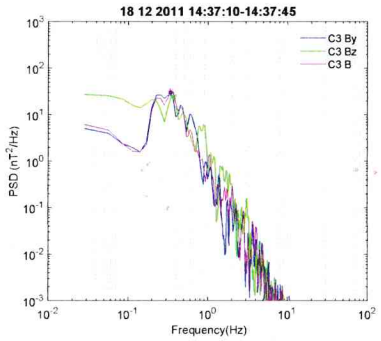

Figure 8. C3 frequency spectra for B_y, B_z components and magnetic field magnitude for shock 18 December 2011.

direction is well defined. The time shift between the magnetic measurements along the maximum variance component is 0.22 s (determined with correlation analysis), while the spacecraft separation along the minimum variance direction is 6.8 km. The resulting wavelength estimate is 61 km for the peak frequency 0.5 Hz. This value is close to spacecraft separation distance (about 40 km) and thus is generally consistent with the observed substantial difference between magnetic fields at C3 and C4.

The hodograph of magnetic field rotation (Fig. 11), however, shows absence of any stable polarization, which can be interpreted as sometimes linear, sometimes circular. The coplanarity approach again can not be used here to confirm the wave vector direction since the angle between the maximum variance direction and the local magnetic field is rather small (20°). The maximum possible wavelength (if spacecraft separation along wave vector is maximal 40 km) is ~400 km.

3.3 Event 3

One more example is from January 3rd, 2008 (14:30–1435 UT) with Cluster separation ~100 km (Table S1, Fig. S3 in Supplement). OMNI data showed very low IMF (1.1 nT) and $\beta = 39$. Solar wind speed is small ~321 km/s, Alfvén Mach number is ≈42, magnetosonic Mach number is ≈7. The model θ_{Bn} is 47°. In Fig. 12 we present a view of local magnetic field along with OMNI data. Though local upstream magnitude is approximately equal to that in OMNI (except starting from 14:30 UT closer to the shock), the upstream field direction ~~is~~ changing by more than 90° and the local model θ_{Bn} ~~is~~ also changing to more perpendicular geometry. The presence of an earlier shock crossing at 14:20 UT may also affect observed upstream conditions. Downstream magnetic field is also strongly changing direction with a temporal scale of about a minute (Fig.12, right side). Therefore for this shock reliable determination of magnetic geometry is impossible. This problem may be inherently related with very small value of upstream magnetic field.

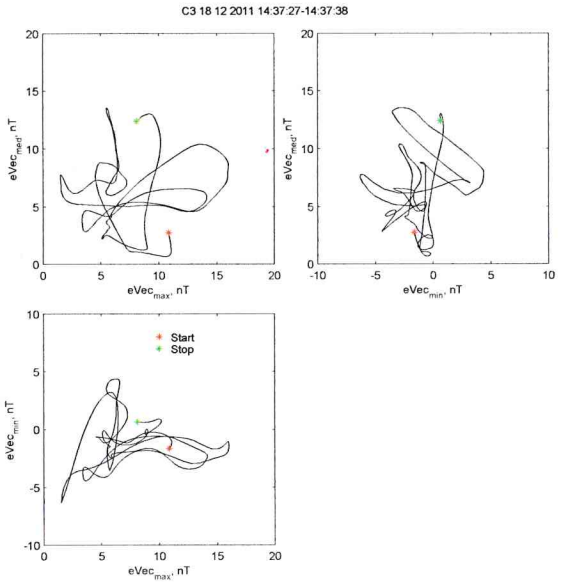

Figure 9. Hodographs of C3 magnetic field in eigenvector coordinates for shock 18 December 2011.

Fig. S3 contains overview of magnetic field and plasma parameters. The transition lasts about 2.5 minutes 14:32:00–14:34:30 UT from the first signs of gyrating ions upstream and growth of parallel ion temperature (Fig. S3e,f) to stable downstream conditions. The jump in magnetic field magnitude is smeared over half a minute 14:34:00–14:34:30 UT, it is wavy rather than step-like and magnetic magnitude downstream is often as small as 1–2 nT. The nominal shock front transition is somewhat arbitrarily placed at 14:34:10 UT (marked by vertical line in Fig.S3). Some increase of variation amplitudes around 14:34:10 UT can be interpreted as a localized front intensification or as a result of shock bounce motion.

Similar to Example 1, one can estimate shock speed along the normal, comparing with C2 crossing (not shown here). The spacecraft separation is 5700–5800 km, while the separation along the model normal is 1400 km. The estimated

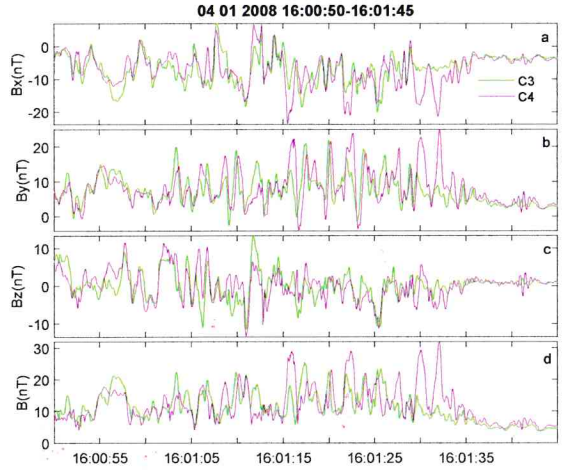

Figure 10. Full resolution magnetic waveform for shock 04 January 2008. In panels (a-d) are components and total value of magnetic field

shock speed is 11 km/s, corresponding to the smeared ramp width about 330 km. The gyroradius of solar wind protons is about 2000 km, the proton inertial length in solar wind is about 80 km.

The detailed view of magnetic variations is in Fig. 13. Only relatively high frequency oscillations about 2 Hz are present (frequency spectra are in Fig. S4). There are no wave packets with the stable phase. For example, at 14:34:10–14:34:14 UT X and Z components are in anticorrelation for C3 and C4, while immediately near, at 14:34:08–14:34:10 UT these components are in phase. Therefore, the reliable multipoint analysis for this event is impossible. Magnetic field hodograph plot for 14:34:10–14:34:14 UT is in Fig.14. It confirms unstable (but consistent with the changing linear) polarization. However, assuming that C3 and C4 variations are mostly in antiphase (half a period between spacecraft), one gets the maximal wavelength estimate ~200 km.

3.4 Observation summary and statistics

Our statistics includes 22 oblique and quasi-perpendicular shocks. The three examples well illustrate typical shock properties. The minimum θ_{Bn} is 37°, two largest ones are 62° and 83°. Values of β range from 39 to 7.5. All cases are supercritical shocks with magnetosonic Mach number more than 5.5. Alfvén Mach numbers are large because of large β. All shocks exhibit

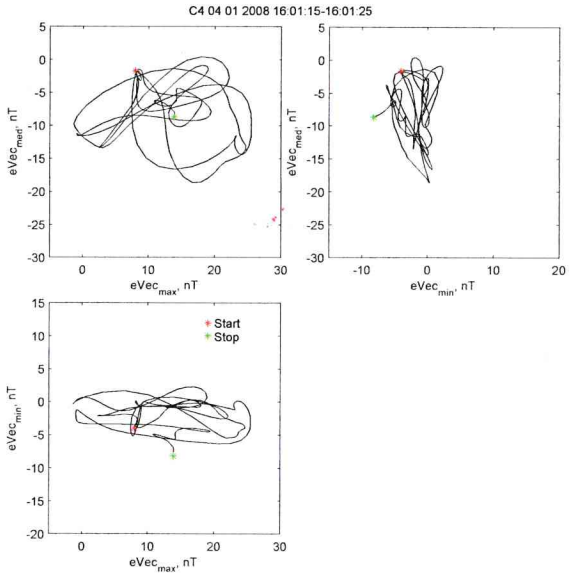

Figure 11. Hodographs of C4 magnetic field in eigenvector coordinates for shock 04 January 2008.

a clear several-minute-long transition zone between pristine solar wind ion flow and magnetosheath. The observed shocks, as concerns their general structure, are typical oblique/quasi-perpendicular shocks, with the somewhat smeared main magnetic field and density increase, which is **about several tens sec long or several hundred km.** This magnetic profile is typical for all our shocks irrespective of θ_{Bn} angle.

On a smaller time scale of seconds, the magnetic profile is dominated by very large amplitude magnetic variations much larger than the background field, which are gradually growing in the course of magnetic field increase towards downstream. As a result, the exact location of the 'main' magnetic jump (aka ramp for supercritical quasi-perpendicular shocks) can not be defined. This presence of high-amplitude variations is in agreement with the previous publications (Winterhalter and Kivelson, 1988).

Table 2. Wave analysis data for shock 04 January 2008, 16:01:15–16:01:25.

max eigenvector, V_{max}	-0.46 0.87 0.17
med eigenvector, V_{med}	0.88 0.42 0.22
min eigenvector, V_{min}	-0.12 -0.25 0.96
eigenvalues	3.4, 22.9, 45.3
magnetic field C3, B_3 (nT)	-9.05, 9.85, -0.75
local proton velocity C4 (km/s)	-178.3, 125.7, -67.4
angle, V_{max} and IMF	46^o
angle, V_{min} and IMF	79^o
angle, V_{max} and B_3	20^o
angle, V_{min} and B_3	99^o
peak frequency in max component	0.5 Hz
time shift in magnetic field along V_{max}	0.22 s
separation along V_{min}	6.8 km
wavelength	61 km

The three examples show characteristics of the dominating magnetic variations, typical for all considered events. The detailed multipoint variation analysis allowed to obtain following new information. In the most of shocks (and in Examples 1 and 2) the variations exhibit the well-defined frequency peak ~0.2–0.5 Hz. The magnetic phase portrait of these variations is irregular, with no clear persistent polarization. It can be also interpreted as a linear polarization with the frequently changing main direction. However since amplitude of variations is larger than the background field, the main axis of linear polarization is always almost along the field vector. Such polarization does not allow to determine reliably the wave propagation direction and the wavelength. We get the estimates only in the range several-tens-hundreds km.

Two shock events (Dec. 31, 2003 and our Example 3, Jan. 3, 2008 14:32 UT) have dominating ~2 Hz variations, visually with more harmonic waveform, but also with the unstable phase. The spatial scale of these variations is smaller than the spacecraft separation, so that it proved to be impossible to determine it with multipoint data. These two shocks are not different from the other events in terms of their other general parameters. Moreover, one of them (Event 3 above) is registered just 10 min after a crossing, which exhibited the first type of variations. Therefore the presence of '2-Hz' waves might be due to some temporal shock front evolution.

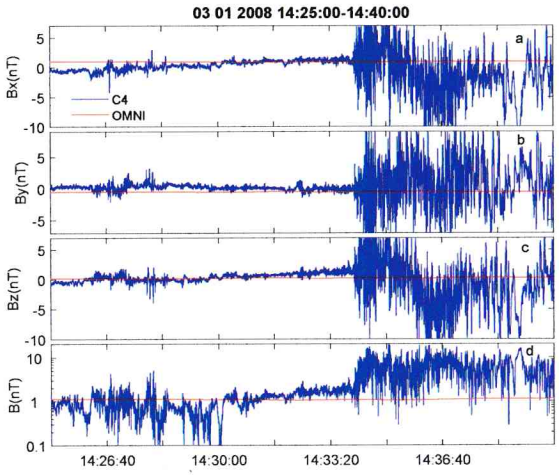

Figure 12. Local upstream and OMNI magnetic field for shock 03 January 2008. In panels (a-d) are components and total value of magnetic field

4 Discussion

4.1 Reliability of solar wind input

High-β solar wind is relatively rare at the Earth orbit. In our study we accepted somewhat ad-hoc threshold of high β equal to 10. Such interplanetary conditions tend to occur during solar minima, being created by slow cold dense solar wind with low IMF (1–2 nT). However is not always easy to confirm that the observed shock crossing actually occurred in high-β solar wind interval, identified in OMNI. The first set of problems is related with association of particular crossings with ~~the~~ stable high β. These problems are relatively straightforward to identify in data. A more substantial problem is related with the inherent solar wind and IMF variability. We measure solar wind in L1 halo orbit, 1.5 million kilometers away from Earth and with halo radius not less than 200 000 km (for ACE spacecraft). A substantial part of modern OMNI data are taken from Wind spacecraft, which is currently on a much wider halo orbit (300–400 thousand km) (Podladchikova et al., 2018). Solar wind and IMF structures at L1 are not necessarily the same that actually affect the magnetosphere. The most questionable is spatial persistence of relatively small changes of IMF from 2 to 1 nT, responsible for creation of very high-β intervals.

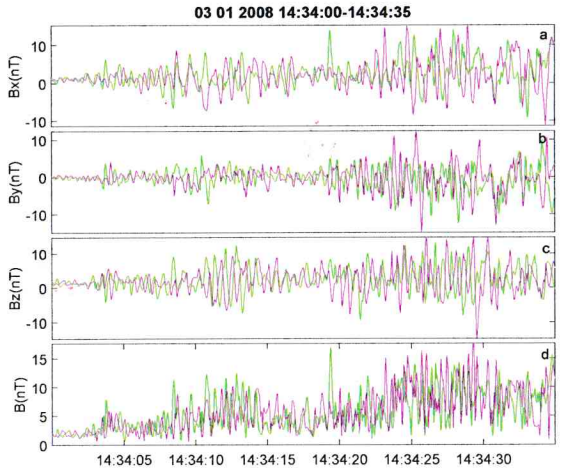

Figure 13. Full resolution magnetic waveform for shock 03 January 2008. In panels (a-d) are components and total value of magnetic field

Though the specific analysis of the spatial scales of high-β areas in solar wind was not performed, available reports indicate significant potential problems. The ISEE data study suggested that during periods of medium to low variance of magnetic field, magnetic features with the scales about 20 R_E perpendicular to the IMF may occur (Crooker et al., 1982). Comparison of L1 Wind and near-Earth Interball data for 1996–1999 have shown (Petrukovich et al., 2001), that the IMF structures, associated with geomagnetic storms (with the threshold of IMF B_z GSM below –10 nT during 3 hours) are practically the same in L1 and the near-Earth orbits. However, about 20–80% of the smaller everyday IMF variations, causing substorms (several nT in magnitude on one-hour scale) are different by more than 25%.

Thus very high β values in OMNI are not readily applicable for a shock study. It is not always possible to check solar wind β immediately before shock crossing. A spacecraft needs to probe pristine solar wind and then rapidly cross the shock, or there should be an additional near-Earth solar wind monitor. Magnetic field can be reliably measured with magnetometer (still assuming offset uncertainty of about 0.1 nT). Accuracy of ion density and temperature measurements is more problematic, since at L1 the specialised thoroughly calibrated instruments are used, while with a magnetospheric spacecraft, calibration could be rougher in solar wind. Assumptions on the constant helium content and constant electron temperature, used while OMNI β calculations, may also result in some errors. **For example, a factor of two change in electron temperature will**

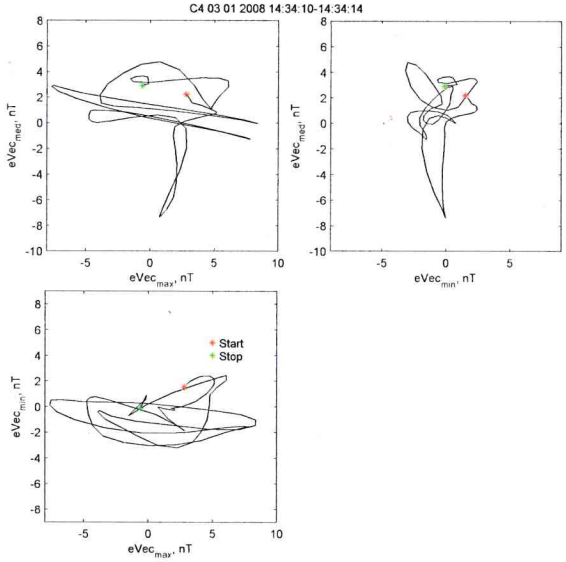

Figure 14. Hodographs of C4 magnetic field in eigenvector coordinates for shock 03 January 2008 for 14:34:10-14:34:14.

result in the change of β by about 30%. Factor of two variations of the He++ content will result in variations of β around 10%. Of course, an additional (relative to those found in the OMNI set) high β intervals may actually form near the bow shock, as a side product of such variability.

4.2 Shock properties

Rather compact large-scale structure of the observed shock transitions is similar to that reported for oblique and quasi perpendicular shocks. It is distinctly different from the structure of quasi-parallel shocks, which ~~are~~ extended up to several Earth radii. However, there are some differences with low-β shocks on a smaller scale. For example the main magnetic and ion density increase in the shock front for all observed events was around several tens of seconds or several hundred km. This scale is larger than proton inertial length, but smaller than ion gyroradius in solar wind. Dependence of shock spatial scale on β is an interesting moment and should be addressed in future studies on larger statistics.

Magnetic variations appear during this ramp-like increase and have the amplitude comparable or larger than the background magnetic field, so that there is no 'stable' magnetic structure on the time scales of seconds. In comparison, for a supercritical quasi-perpendicular low-β shock, one usually defines, starting from the upstream, the prolonged interval of somewhat enhanced density and magnetic field (shock foot, lasting tens of seconds) and the sharp main increase (ramp, lasting seconds). The ramp is often used to determine the shock motion with multipoint measurements, but in our case it is impossible. The increased width of main magnetic jump and its wavy nature might be related with some essential scales in the high-β plasma (large ion gyro radius) or be a sign of an unstable cyclically reforming shock (e.g., Lefebvre et al., 2009). A more detailed phenomenological description of this shock transition requires analysis of ion kinetics, which will be performed elsewhere.

Observed shock crossings in their general appearance, in particular, with the presence of high-amplitude magnetic variations and absence of clear ramp profile, are similar to those earlier presented by Formisano et al. (1975) and Farris et al. (1992) (as far as it can be discerned with visual examination of figures). In this study we advance our knowledge, determining some quantitative features of those variations.

4.3 Magnetic variation properties

Observed properties of low-frequency magnetic variations (linear polarization with very high amplitude, substantially changing the total magnetic field) suggest their strong non-linearity and compressive nature. Absence of any several-periods-long wave packets with the stable phase also suggest strong spatial localisation.

With two Cluster spacecraft separated by several tens km it was possible to estimate the spatial scale of these dominating variations. Three typical variants were found. In some events (Example 1) variations had rather irregular form, typical frequency of about 0.5 Hz, and were very similar on two spacecraft, suggesting the scale of some hundred km. The wavelength can be determined independently to propagation direction only with four measuring points, unlike our cases. Alternatively one can fix propagation direction with the minimum variance analysis in the case of elliptic polarization or with the coplanarity supposition. Unfortunately in our cases it proved ~~to be~~ impossible to determine

the wavevector direction reliably by ~~both~~ methods, since we have linearly polarized waves with maximum variance direction along the main magnetic field. Note, that such configuration is inevitable for a variation much larger than the background field.

The second variant of a spatial scale is illustrated with Example 2. It includes the variations visually similar to that in Example 1, but with a mix of scales of the order of hundred km, which can be captured with our spacecraft separation, and of the order of tens km. As a result, the waveforms are rather different, but common features can sometimes be traced. Finally, the third variant (Example 3) contains more harmonic waves with higher frequencies around 1–2 Hz and the unresolved dominating spatial scale of at most 200 km.

The observed variations are ~~strongly~~ different from that in low-β supercritical events (e.g. Krasnoselskikh et al., 2013), where clear whistler wave packets with elliptic polarization dominate. Observed polarization is also not consistent with the Alfvén mode, earlier suggested for high-β shock (Coroniti, 1970; Kennel and Sagdeev, 1967).

Dominating downstream wave mode was also addressed in a number of other investigations, however cases of really high $\beta > 10$ were not specifically addressed. Hubert et al. (1989) identified the mirror waves, comparing magnetic field with density, provided by the fast electron measurements of ISEE project. Balikhin et al. (1997) identified the intermediate mode with two-point AMPTE data analysis. Lacombe et al. (1992) suggested for higher-β shocks the mirror mode with linear polarization, and successfully used coplanarity assumption to define the wavevector direction. Czaykowska et al. (2001) have shown compressive mode as well as left-hand polarized mode in shocks with $\beta > 1$. Therefore, almost full variety of possible wave mode variants was identified. A definite plasma mode analysis critically depends on reliable determination of the wave propagation (wavevector) direction, which proved to be impossible in our cases. Also, it should be noted, that all studies referenced above, used several-minute data intervals, which were often several minutes away from the shock transition. In the most of cases, the analysed frequencies were below 0.1 Hz. This approach is different from ours, we addressed relatively short intervals of the most powerful oscillations.

Though some of the above-cited studies addressed 'higher-β' shocks, actually their statistics was definitely dominated with $\beta \geq 1$ cases. The only published cases with really high β (Formisano et al., 1975; Winterhalter and Kivelson, 1988; Farris et al., 1992) were not accompanied with any plasma mode analysis, however visually the wave actitvity in these events were similar to our Examples 1 and 2.

An alternative wave mode candidate, frequently suggested for high-β plasma, is Weibel instability, which is fundamentally similar to drift mirror mode. With no seed magnetic field the Weibel mode has only imaginary frequency. The latter means that the magnetic field clamps are growing faster, than propagate. For finite magnetic field Pokhotelov and Balikhin (2012) suggested, that Weibel mode grows as a mix of two opposite circular polarizations, attains some small real part of frequency. Thus in some features (linear polarization, chaotic phase) it is consistent with observations.

5 Conclusions

High-β ($\beta > 10$) shocks are relatively rare and largely unexplored class of Earth bow shock. Formation of high-β interplanetary plasmas is mostly related with dense slow solar wind and very low magnetic field up to 1–2 nT. **Due to spatial variability of low IMF, it is ~~more~~ difficult to determine shock geometry for higher β (in OMNI) cases. However at some (large) β shock structure should become independent from magnetic field direction. This is an interesting direction of future studies.**

Our statistics includes oblique and quasi-perpendicular shocks. The main magnetic field and ion density jumps in the shock fronts are smeared to several hundred km, so the overall ~~layout~~ is quite characteristic and distinctly different from that for quasi-parallel and supercritical quasi-perpendicular shocks.

Dominating magnetic variations have amplitudes much larger than the background field, frequencies 0.2–0.5 Hz, sometimes, ~2 Hz. Polarization is mostly irregular and close to linear, the spatial scales range from several tens to couple hundred km. These properties are definitely different from that for fast magnetosonic or Alfvén modes earlier reported for some other shock types. In some features the variations may be consistent with the Weibel instability, but observations with more closely spaced spacecraft are necessary to conclude more definitely on the wave mode.

Author contributions. OMC and PIS performed the data processing and analysis. AAP is responsible for data analysis and interpretation. AAP prepared the manuscript with contributions from all co-authors.

Competing interests. The authors declare that they have no conflict of interest.

Acknowledgements. The data analysis was funded with Russian Science Fund project 05-14-00824. We are thankful for Cluster Science Archive, CDAWeb and OMNI for availability of spacecraft data.